www.ietdl.org

Published in IET Generation, Transmission & Distribution
Received on 15th August 2012
Revised on 22nd September 2012
Accepted on 10th October 2012
doi: 10.1049/iet-gtd.2012.0186

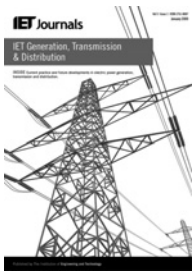

ISSN 1751-8687

# Hourly demand response in day-ahead scheduling for managing the variability of renewable energy

*Hongyu Wu[1], Mohammad Shahidehpour[1,2], Ahmed Al-Abdulwahab[2]*

[1]*Department of Electrical and Computer Engineering, Robert W. Galvin Center for Electricity Innovation, Illinois Institute of Technology, Chicago, IL, USA*
[2]*Department of Electrical and Computer Engineering, King Abdulaziz University, Jeddah, Saudi Arabia*
*E-mail: ms@iit.edu*

**Abstract:** This study proposes a stochastic optimisation model for the day-ahead scheduling in power systems, which incorporates the hourly demand response (DR) for managing the variability of renewable energy sources (RES). DR considers physical and operating constraints of the hourly demand for economic and reliability responses. The proposed stochastic day-ahead scheduling algorithm considers random outages of system components and forecast errors for hourly loads and RES. The Monte Carlo simulation is applied to create stochastic security-constrained unit commitment (SCUC) scenarios for the day-ahead scheduling. A general-purpose mixed-integer linear problem software is employed to solve the stochastic SCUC problem. The numerical results demonstrate the benefits of applying DR to the proposed day-ahead scheduling with variable RES.

## Nomenclature

### *Parameters*

| | |
|---|---|
| $N_T$ | number of time periods |
| $N_G$ | number of available generators |
| $N_B$ | number of buses |
| $N_D$ | number of renewable energy sources |
| $N_J$ | number of batteries |
| $N_S$ | number of scenarios |
| $t$ | index for time periods, $t = 1, 2, \ldots, N_T$ |
| $i$ | index for generators, $i = 1, 2, \ldots, N_G$ |
| $b$ | index for buses, $b = 1, 2, \ldots, N_B$ |
| $k$ | index for renewable sources, $k = 1, 2, \ldots, N_D$ |
| $j$ | index for batteries, $j = 1, 2, \ldots, N_J$ |
| $s$ | index for scenarios, $s = 1, 2, \ldots, N_S$ |
| $l$ | index for available transmission lines |
| $\mathrm{NB}^D_{b,t}$ | number of blocks of energy demand by bus $b$ at time $t$ |
| $\mathrm{NB}^G_{i,t}$ | number of blocks of supply bid offered by generator $i$ at time $t$ |
| $P_s$ | probability of scenario $s$ |
| $\mathrm{NL}_i$ | no-load cost of generator $i$, in \$ |
| $\lambda D_{n,b,t}$ | marginal benefit of the $n$th block of the bid at bus $b$ and time $t$, in \$/MW |
| $\lambda G_{m,i,t}$ | marginal production cost of the $m$th block of generator $i$ at time $t$, in \$/MW |
| $\mathrm{VOLL}_{b,t}$ | value of lost load at bus $b$ at time $t$, in \$ |
| $\mathrm{RCAP}_t$ | system reserve requirement at time $t$, in MW |
| $P^{\max}_i$ | upper generation limit of unit $i$, in MW |
| $\Gamma^{(\cdot)}_{(\cdot)}$ | shift factor |
| $\mathrm{DR}^{\min}_{b,t}$ | minimum curtailed load at bus $b$ and time $t$, in MW |
| $\mathrm{DR}^{\max}_{b,t}$ | maximum curtailed load at bus $b$ and time $t$, in MW |
| $D^{\max}_{b,t}$ | maximum load at bus $b$ at time $t$, in MW |
| $\Delta G_i$ | maximum ramp up/down rate of generator $i$, in MW/min |
| $\Delta D_b$ | pick-up or drop-off rate of load at bus $b$ |
| $X^{\mathrm{on}}_{b,t-1}$ | ON time of load at bus $b$ at time $t-1$, in hour |
| $X^{\mathrm{off}}_{b,t-1}$ | OFF time of load at bus $b$ at time $t-1$, in hour |
| $\mathrm{UT}_b$ | minimum ON time of load at bus $b$, in hour |
| $\mathrm{DT}_b$ | minimum OFF time of load at bus $b$, in hour |
| $E^{\max}_b$ | maximum energy change at bus $b$ in the scheduling horizon, in MW |
| $\underline{q}^c_j$ | minimum charge of storage $j$, in MW |
| $\bar{q}^c_j$ | maximum charge of storage $j$, in MW |
| $\underline{q}^d_j$ | minimum discharge of storage $j$, in MW |
| $\bar{q}^d_j$ | maximum discharge of storage $j$, in MW |
| $\underline{e}_j$ | minimum state of storage $j$, in MW |
| $\bar{e}_j$ | capacity of storage $j$, in MW |
| $\tau$ | reserve responsive time, usually in 10 minutes |
| $\eta$ | period span, usually in hour |
| $\lambda_{(\cdot)}$ | mean time to failure for system component, in hour |
| $\mu_{(\cdot)}$ | mean time to repair for system component, in hour |

### *Variables*

| | |
|---|---|
| $d^s_{n,b,t}$ | demand in the $n$th block of the stepwise demand bid at bus $b$ at time $t$ in scenario $s$, in MWh |

$p^s_{m,i,t}$ generation in the $m$th block of piecewise linear output by generator $i$ at time $t$ in scenario $s$, in MW
$S_{i,t}(\cdot)$ start-up or shut-down cost of unit $i$ at time $t$, in \$
$X_{i,t}$ time periods when unit $i$ has been ON or OFF at time $t$, in hour
$DL^s_{b,t}$ loss of load at bus $b$ at time $t$ in scenario $s$, in MW
$p^s_{i,t}$ dispatch of generator $i$ at time $t$ in scenario $s$, in MW
$g^s_{k,t}$ dispatch of renewable source $k$ at time $t$ in scenario $s$, in MW
$q^s_{j,t}$ charge ( − ) or discharge ( + ) of storage $j$ at time $t$ in scenario $s$, in MW
$C^s_{j,t}$ state of charge (SOC) of storage $j$ at time $t$ in scenario $s$, in %
$DE_{b,t}$ expected price-responsive load at bus $b$ at time $t$, in MW
$DB^s_{b,t}$ customer base load at bus $b$ at time $t$ in scenario $s$, in MW
$DR^s_{b,t}$ adjustable load of bus $b$ at time $t$ in scenario $s$, in MW
$RU^s_{i,t}$ reserve provided by generator $i$ at time $t$ in scenario $s$, in MW
$RB^s_{j,t}$ reserve provided by storage $j$ at time $t$ in scenario $s$, in MW
$z_{i,t}$ commitment status of thermal generator $i$ at time $t$; 1 for ON and 0 for OFF
$y^s_{b,t}$ state of curtailment at bus $b$ at time $t$ in scenario $s$; 1 when curtailed and 0 otherwise

## 1 Introduction

The hourly demand response (DR) program in electricity markets could provide significant benefits to market participants and customers. Such benefits include lower hourly market prices, lower volatility in hourly market prices, enhanced system reliability and a smaller chance for the market power exertion by generating companies (GENCO), as customers play a more active role in power system operations. DR offers incentives for lowering electricity usage at times when electricity prices are high or when the power system reliability is in question [1–3]. DR becomes more attractive to customers and ISOs as electricity demands, fuel prices and the quest for achieving a higher system reliability increase.

The DR program includes reliability and economic considerations. In the reliability DR program, participating customers are paid incentives for measured baseline load reductions during contingency conditions [2]. In the economic DR program, participating consumers would curtail hourly loads voluntarily in response to market prices. In this case, customers would shift their less critical hourly loads to periods that would balance potential cost savings against customer inconvenience [4–8]. The efficient market dynamics are represented by incorporating both economic and reliability DR programs into the market clearing process.

The integration of renewable energy sources (RES) into power systems could reduce transmission losses and congestion by dispersing power generation, improve the system reliability, defer infrastructure upgrades by the installation of local power supply, reduce carbon footprint by customising the use of RES and improve the system efficiency by enhancing the power quality according to customer requirements [9–11]. However, the widespread usage of variable RES could be problematic for power system operations [12, 13].

The simulation-based approach is generally applied when considering RES. A set of power production scenarios with their probabilities is introduced to handle uncertainties [14]. The stochastic unit commitment and dispatch with high wind penetration are examined for rolling planning with scenario trees [15]. Rolling planning is carried out for rescheduling which is based on the most up-to-date wind forecasts and existing schedules [16]. A methodology is proposed to determine the required level of spinning and non-spinning reserves with a high penetration of wind power [17]. The Monte Carlo simulation (MCS) method is applied to evaluate the performance of grid-connected wind turbine generators (WTGs) [18, 19]. WTGs are modelled as energy-limited units by using a load modification technique [20]. Reliability indices are developed for hybrid solar-wind generation systems [21].

This paper proposes a short-term stochastic security-constrained unit commitment (SCUC) model for day-ahead markets, which incorporates a coordinated DR and storage program for managing variable RES, random outages of generating units and transmission lines, and load and wind forecast errors. Both economic and reliability DR programs are considered in the presented DR model. The operating characteristics of loads include stepwise price bids and physical constraints of loads. The scenario reduction is adopted in MCS as a tradeoff between calculation speed and solution accuracy. A general-purpose mixed-integer linear problem (MILP) software is employed to solve the stochastic SCUC problem.

The rest of paper is organised as follows: The market-clearing mechanism is provided in Section 2. The MCS method for simulating the stochastic SCUC is described in Section 3. The mathematical formulation of the stochastic SCUC problem is proposed in Section 4. Numerical testing results are presented and analysed in Section 5. The observation and the concluding remarks are provided in Sections 6 and 7, respectively.

## 2 Proposed market-clearing mechanism

### 2.1 Day-ahead market

The ISO received bids from market participants including load aggregators and DR providers, and clears the market by optimising the hourly dispatch of individual generating units over a scheduling horizon. The day-ahead schedule will maximise the social welfare while satisfying system-wide limits and operating constraints of individual market participants.

### 2.2 DR program

In the proposed DR model, loads include the customer base load (CBL) and the price responsive load (PRL). CBL is forecasted based on the historical data; for example, the customer's average electricity usage in the curtailment bid period during the 10 days prior to the day when the bid was submitted [22]. The economic DR may include blocks of hourly PRL bids with corresponding prices. The hourly constraints may include expected PRL, minimum/maximum curtailable load, maximum load pick-up/drop-off rate and minimum up/down time of load curtailment. PRL can be curtailed or shifted to other time periods for economic reasons as scheduled by ISO in the day-ahead market. The proposed model allows customers to participate in reliability DR program. The CBL of participating customers could be curtailed in the case of a system emergency. Customers are required to submit the maximum loss of load and the value of lost load (VOLL) to the DA market and the load

curtailment will be scheduled by ISO. Unlike the PRL in economic DR, the loss of load is involuntary [23, 24]. If load shedding occurs, customers will get compensated equivalent to the amount of lost load multiplied by the corresponding VOLL.

Both DR programs offer operation reserves to the ancillary service market. The energy and reserve markets are scheduled and cleared simultaneously through MILP in the proposed model.

## 3 MCS for stochastic SCUC

The stochastic SCUC in our proposed model includes the following:

### 3.1 Renewable energy sources

We disregard for simplicity the correlation of load and RES and treated them independently in the scheduling horizon. Suppose the random photovoltaic array (PVA) output follows a Beta distribution and the random WTG output follows a Weibull distribution at each time period [25]. The continuous probability distribution functions (PDFs) are approximated by a discrete distribution. Let $\mathrm{PVA}_t$ and $\mathrm{WTG}_t$ denote discrete probability distributions for PVA and WTG outputs at time $t$, respectively. Then

$$\mathrm{PVA}_t = \left[\left\{s_t^n, P\left(s_t^n\right)\right\}\right], \quad n = 1, 2, \ldots, \mathrm{NS}_t \tag{1}$$

$$\mathrm{WTG}_t = \left[\left\{w_t^n, P\left(w_t^n\right)\right\}\right], \quad n = 1, 2, \ldots, \mathrm{NW}_t \tag{2}$$

where $\mathrm{NS}_t$ and $\mathrm{NW}_t$ are the total number of discrete output levels in $\mathrm{PVA}_t$ and $\mathrm{WTG}_t$, respectively; $s_t^n$ and $w_t^n$ are the $n$th discrete levels of PVA and WTG outputs at time stage $t$, respectively; $P\left(s_t^n\right)$ and $P\left(w_t^n\right)$ are probabilities of occurrence with respect to $s_t^n$ and $w_t^n$, which can be calculated based on their probability density functions (PDFs).

We divide the entire scheduling horizon into several time stages in which each stage spans several hours. For each time stage, several scenarios are created based on historical data in which PVA and WTG outputs are different from the corresponding forecasts. The probability of each scenario at each stage is calculated as its weight is based on the PDF. The weight for the final-stage scenario is obtained by multiplying corresponding weights along the scenario tree. The stochastic output of PVA or WTG is then represented by possible scenarios with their corresponding probability.

### 3.2 Monte Carlo simulation

The number of samples needed for a given accuracy level is irrelevant to the system size; so the MCS method is suitable for representing the uncertainty in large-scale optimisation problems. MCS includes random outages of generating units and transmission lines [26, 27] as well as CBL forecast errors which represent variations around the forecasts at each time stage. The CBL forecast errors are represented by normal distribution functions in which the mean values are the forecasts and the standard deviations are percentages of the mean values. The outages of generator and transmission line are simulated based on forced outage rates and repair rates [27]. In each scenario, a sampling method [26] is used to determine the 0/1 value of system component availability. Scenario reduction is adopted as a tradeoff between computational burden and modelling accuracy in large-scale DR scheduling problems [28]. The probability metrics based on the scenario reduction method is applied.

## 4 Stochastic problem formulation and constraints

We assume electricity market participants are independent bidders who bid at their respective marginal costs. ISO calculates the hourly SCUC and DR schedule, and hourly locational marginal prices (LMPs). The problem objective and constraints are formulated as follows.

### 4.1 Objective function

The objective of the proposed SCUC problem is to determine the day-ahead hourly schedule of generating units and hourly DR schedule such that the expected total social welfare is maximised. The social welfare is defined as the sum of consumer surplus and the producer surplus as shown in Fig. 1. The objective function is expressed as follows

$$\begin{aligned}\max \quad & \sum_{s=1}^{N_S} P_s \left\{ \sum_{t=1}^{N_T} \sum_{b=1}^{N_B} \sum_{n=1}^{\mathrm{NB}_{b,t}^D} \lambda D_{n,b,t} d_{n,b,t}^s \right. \\ & - \sum_{t=1}^{N_T} \sum_{i=1}^{N_G} \left[ \sum_{m=1}^{\mathrm{NB}_{i,t}^G} \lambda G_{m,i,t} p_{m,i,t}^s + \mathrm{NL}_i z_{i,t} + S_{i,t}\left(X_{i,t}, z_{i,t}\right) \right] \\ & \left. - \sum_{t=1}^{N_T} \sum_{b=1}^{N_B} \mathrm{VOLL}_{b,t} \mathrm{DL}_{\mathrm{b,t}}^s \right\}\end{aligned} \tag{3}$$

The first term in the objective function (3) is the customer gross surplus and the second term is the generation cost of thermal units, which includes fuel cost, no-load cost and piecewise linear start-up and shut-down cost. The third term represents the cost of load curtailment. The objective is subject to the following individual scenario constraints.

### 4.2 System and unit constraints

Constraints (4), (6) and (8) are on power balance, system reserve and transmission flows, respectively. Constraints (5) and (7) show unit spinning reserve and line flows, respectively. Other physical constraints of generating units are generating unit limits, ramp rate limits and min up/down

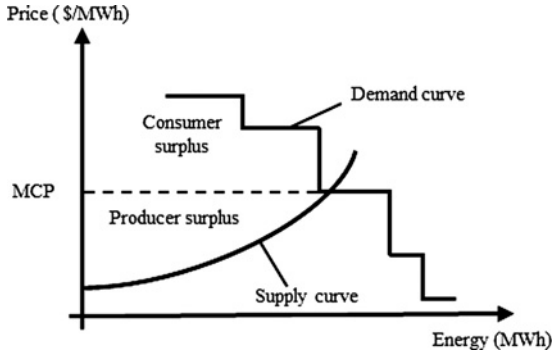


**Fig. 1** *Net social welfare and market equilibrium*




doi: 10.1049/iet-gtd.2012.0186

time limits [1, 29, 30].

$$\sum_{i=1}^{N_G}\sum_{m=1}^{\mathrm{NB}_{i,t}^{G}} p_{m,i,t}^{s} + \sum_{k=1}^{N_D} g_{k,t}^{s} + \sum_{j=1}^{N_J} q_{j,t}^{s} - \sum_{b=1}^{N_B}\left(\mathrm{DE}_{b,t} - \mathrm{DR}_{b,t}^{s}\right) = 0, \quad \forall t, \forall s \tag{4}$$

$$\mathrm{RU}_{i,t}^{s} = z_{i,t}\cdot\min\left\{P_i^{\max} - p_{i,t}^{s}, \Delta G_i\cdot\tau\right\}, \quad \forall i, \forall t, \forall s \tag{5}$$

$$\sum_{i=1}^{N_G}\mathrm{RU}_{i,t}^{s} + \sum_{j=1}^{N_J}\mathrm{RB}_{j,t}^{s} + \sum_{b=1}^{N_B}\mathrm{DR}_{b,t}^{s} \geq \mathrm{RCAP}_t, \quad \forall t, \forall s \tag{6}$$

$$F_{l,t}^{s} = \sum_{i=1}^{N_G}\Gamma_{l,i}^{G}\sum_{m=1}^{\mathrm{NB}_{i,t}^{G}} p_{m,i,t}^{s} + \sum_{k=1}^{N_D}\Gamma_{l,k}^{D} g_{k,t}^{s} + \sum_{j=1}^{N_J}\Gamma_{l,j}^{J} q_{j,t}^{s} - \sum_{b=1}^{N_B}\Gamma_{l,b}^{L}\left(\mathrm{DE}_{b,t} - \mathrm{DR}_{b,t}^{s}\right), \quad \forall l, \forall t, \forall s \tag{7}$$

$$-\bar{F}_l \leq F_{l,t}^{s} \leq \bar{F}_l, \quad \forall l, \forall t, \forall s \tag{8}$$

### 4.3 DR constraints

Fig. 2 shows a stepwise DR bid in which OA, OC and OD represent the CBL, the expected PRL, and the maximum hourly load, respectively. CB and CF are the minimum and maximum load curtailment, respectively. OE denotes the customer load scheduled by ISO in the day-ahead market. Point E (end point of the scheduled load) would be located within two zones of FB and CD as highlighted in Fig. 2. The PRL can be curtailed or shifted to another time period for satisfying system economic or reliability constraints. The ratio of available PRL to the expected PRL is defined as load participation factor (LPF), which is expressed as LPF = AC/OC in Fig. 2. A higher LPF indicates a higher price elasticity of demand and more curtailable loads. $\mathrm{DR}_{b,t}^{s}$ is the adjustable load of bus $b$ at time $t$ in scenario $s$ which is calculated as the difference between the expected PRL and the scheduled load as shown in Fig. 2. The decision variables in the proposed DR model are $\mathrm{DR}_{b,t}^{s}$ and its 0–1 state. $\mathrm{DR}_{b,t}^{s}$ is positive when the load is shifted out from bus $b$ at time $t$, and negative when the load is shifted to bus $b$ at time $t$.

The DR constraints are listed in (9)–(15). The correlation between block demand and total demand is given in (9). The limit on curtailable load is provided in (10), which may either reflect physical load limits or be imposed by ISO.

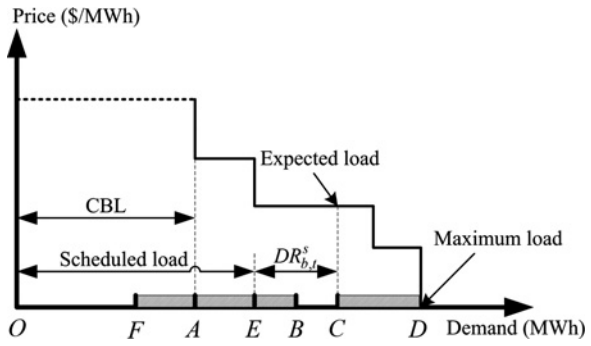


**Fig. 2** *Stepwise demand response bid*

The loss of load constraint is shown in (11), which indicates that loss of load could occur if and only if all PRLs are completely curtailed. Limits on pick-up/drop-off rate of load, min up/down time for load curtailment and allowable change of bus load across schedule horizon are given in (12)–(15), respectively. Constraint (12) would restrict the rate of customer load changes between any two successive hours. Constraint (13) indicates the minimum number of hours that a load would be curtailed. Constraint (14) shows the minimum number of hours when the load would be supplied. Constraint (15) would limit the total number of load curtailments in the scheduling horizon. By setting $E_b^{\max}$ to 0 in (15), the curtailed load at certain time periods will be fully shifted to other periods.

$$\sum_{n=1}^{\mathrm{NB}_{b,t}^{D}} d_{n,b,t}^{s} = \mathrm{DE}_{b,t} - \mathrm{DR}_{b,t}^{s}, \quad \forall b, \forall t, \forall s \tag{9}$$

$$\begin{cases} \mathrm{DR}_{b,t}^{\min} y_{b,t}^{s} \leq \mathrm{DR}_{b,t}^{s} \leq \mathrm{DR}_{b,t}^{\max} y_{b,t}^{s}, & \text{if} \quad \mathrm{DR}_{b,t}^{s} \geq 0 \\ \mathrm{DR}_{b,t}^{s} \geq \mathrm{DE}_{b,t} - D_{b,t}^{\max}, & \text{else} \end{cases} \quad \forall b, \forall t, \forall s \tag{10}$$

$$\mathrm{DL}_{b,t}^{s} = \max\left\{\mathrm{DB}_{b,t}^{s} - \left(\mathrm{DE}_{b,t} - \mathrm{DR}_{b,t}^{s}\right), 0\right\}, \quad \forall b, \forall t, \forall s \tag{11}$$

$$\left|\left(\mathrm{DE}_{b,t} - \mathrm{DR}_{b,t}^{s}\right) - \left(\mathrm{DE}_{b,t-1} - \mathrm{DR}_{b,t-1}^{s}\right)\right| \leq \Delta D_b, \quad \forall b, \ t = 2, 3, \ldots, N_T, \forall s \tag{12}$$

$$\left(X_{b,t-1}^{s,\mathrm{on}} - \mathrm{UT}_b\right)\left(y_{b,t-1}^{s} - y_{b,t}^{s}\right) \geq 0, \quad \forall b, t = 2, 3, \ldots, N_T, \forall s \tag{13}$$

$$\left(X_{b,t-1}^{s,\mathrm{off}} - \mathrm{DT}_b\right)\left(y_{b,t}^{s} - y_{b,t-1}^{s}\right) \geq 0, \quad \forall b, t = 2, 3, \ldots, N_T, \forall s \tag{14}$$

$$0 \leq \sum_{t=1}^{N_T}\mathrm{DR}_{b,t}^{s} \leq E_b^{\max}, \quad \forall b, \forall t, \forall s \tag{15}$$

### 4.4 Storage constraints

We assume the power system is equipped with a storage with the following constraints: input and output limits of storage, SOC dynamics, SOC limits, initial/final SOC and reserve contribution of storage are given in (16)–(20), respectively [31]. In (16), $q_{j,t}^{s}$ is negative when storage is charging, positive when the storage is discharging and 0 when the storage is not functional. Constraint (20) indicates that reserve provided by storage is the minimum of its existing capacity and the maximum discharge.

$$q_{j,t}^{s} \in \left\{0, \left[-\bar{q}_j^{c}, -\underline{q}_j^{c}\right], \left[\underline{q}_j^{d}, \bar{q}_j^{d}\right]\right\}, \quad \forall j, \forall t, \forall s \tag{16}$$

$$C_{j,t}^{s} = C_{j,t-1}^{s} - q_{j,t}^{s}\cdot\eta/\bar{e}_j, \quad \forall j, \forall t = 2, 3, \ldots, N_T, \forall s \tag{17}$$

$$\underline{C}_j = \frac{\underline{e}_j}{\bar{e}_j} \le C^s_{j,t} \le 1, \quad \forall j, \forall t, \forall s \tag{18}$$

$$C^s_{j,0} = C^0_j, \; C^s_{j,T} = C^T_j, \quad \forall j, \forall s \tag{19}$$

$$\mathrm{RB}^s_{j,t} = \tau \cdot \min\left\{C^s_{j,t} * \bar{e}_j, \bar{q}^d_j\right\}, \quad \forall j, \forall t, \forall s \tag{20}$$

Here, (4)–(20) are constraints that are related to individual scenarios. In each scenario, the availability of system components is represented by a set of input parameters in the proposed optimisation formulation. For the purpose of presentation, this additional set of variables is not introduced in the SCUC formulation. Thermal units are formulated as non-quick start units with hourly scenario commitments which are the same as those in the base case. However, the dispatch of individual committed thermal units in scenarios could be altered in response to scenario realisations. The final dispatch of a thermal unit is its expected dispatch which is the corresponding weighted average solution of all possible scenarios.

## 5 Numerical solution for the proposed problem

Numerical cases are studied for a modified 6-bus system and a modified IEEE 118-bus system. The MILP model (3)–(20) is solved using the ILOG CPLEX 11.0 [32] in Microsoft Visual C# .NET on an Intel Xeon Server with 64 GB RAM. The DR program is implemented at all load buses and curtailed load will be shifted to other periods. The hourly PRLs consist of a single energy block with a bidding price of 20 $/MWh. The system reserve requirement is set as the largest generating unit capacity.

### 5.1 Modified 6-bus system

The modified 6-bus system, shown in Fig. 3, has three thermal units, one WTG, and seven transmission lines. The characteristics of generators, transmission lines and the expected hourly loads are listed in Tables 1–3, respectively.

Three cases are studied to illustrate the impact of DR program on the RES variability in the day-ahead scheduling:

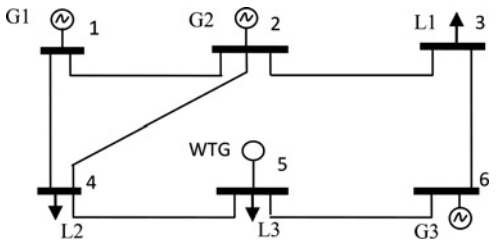


**Fig. 3** *One line diagram of 6-bus system*

**Table 2** Transmission line data for 6-bus system

| Line no. | From bus | To bus | X, pu | Flow limit, MW | $\lambda_l$, h | $\mu_l$, h |
|---|---|---|---|---|---|---|
| 1 | 1 | 2 | 0.170 | 200 | 23.5 | 0.5 |
| 2 | 1 | 4 | 0.258 | 100 | 23.7 | 0.3 |
| 3 | 2 | 3 | 0.037 | 100 | 23.6 | 0.4 |
| 4 | 2 | 4 | 0.197 | 100 | 23.6 | 0.4 |
| 5 | 3 | 6 | 0.018 | 100 | 23.7 | 0.3 |
| 6 | 4 | 5 | 0.037 | 100 | 23.6 | 0.4 |
| 7 | 5 | 6 | 0.140 | 100 | 23.8 | 0.2 |

**Table 3** Expected hourly load for 6-bus system

| H | Load, MWh | H | Load, MWh | H | Load, MWh | H | Load, MWh |
|---|---|---|---|---|---|---|---|
| 1 | 175.19 | 7 | 168.39 | 13 | 242.18 | 19 | 245.97 |
| 2 | 165.15 | 8 | 177.60 | 14 | 243.60 | 20 | 237.35 |
| 3 | 158.67 | 9 | 186.81 | 15 | 248.86 | 21 | 237.31 |
| 4 | 154.73 | 10 | 206.96 | 16 | 255.79 | 22 | 215.67 |
| 5 | 155.06 | 11 | 228.61 | 17 | 256.00 | 23 | 185.93 |
| 6 | 160.48 | 12 | 236.10 | 18 | 246.74 | 24 | 195.60 |

Case 1: DR is considered at all load buses.
Case 2: Combined DR and WTG variability is considered.
Case 3: Effect of DR, WTG variability and storage on hourly LMPs is compared.

These cases are discussed as follows:

*Case 1*: Economic DR program is considered at all load buses. Fig. 4 shows the hourly system demand with several LPFs. At peak hours, the hourly load profile will be more flat as LPF increases. In Fig. 4, the load profile with LPF = 0.3 is almost flat during Hours 6–24, and the standard deviation of hourly load is reduced from 101 to 18 MW at 0.3 LPF. A flat load profile corresponds to lower LMPs, lower transmission congestion and lower system production cost. Also, power system operations will be more efficient since the hourly demand fluctuations are less frequent [2]. We assume a large WTG is located at Bus 5 with its deterministic hourly profile shown in Fig. 5. With a higher LPF, the system load profile will be increasingly close to the WTG profile. In an extreme case, when LPF = 0.9, the system load profile would almost match that of WTG in which the peak load is shifted to other hours when the WTG output reaches its peak.

*Case 2*: In this case, economic DR at all load buses and variable WTG output at Bus 5 are included. The forecasted hourly WTG output is based on http://www.nrel.gov/. The 24-hour scheduling horizon is divided into four time stages when each time stage spans 6 hours. For each time stage, five scenarios including the forecasted output are considered in which the probability of each scenario is calculated according to the PDF of Weibull distribution. For simplicity, the variance is fixed during the horizon. There are $5^4 = 625$ scenarios and each scenario represents a possible WTG

**Table 1** Generators' data for 6-bus system

| U | $P_{max}$, MW | $P_{min}$, MW | Initial status, h | Min down, h | Min up, h | Ramp, MW/h | $\lambda_i$, h | $\mu_i$, h |
|---|---|---|---|---|---|---|---|---|
| G1 | 220 | 100 | 4 | 4 | 4 | 30 | 23.6 | 0.4 |
| G2 | 100 | 10 | −3 | 3 | 2 | 50 | 23.7 | 0.3 |
| G3 | 20 | 10 | −1 | 1 | 1 | 20 | 23.8 | 0.2 |




doi: 10.1049/iet-gtd.2012.0186

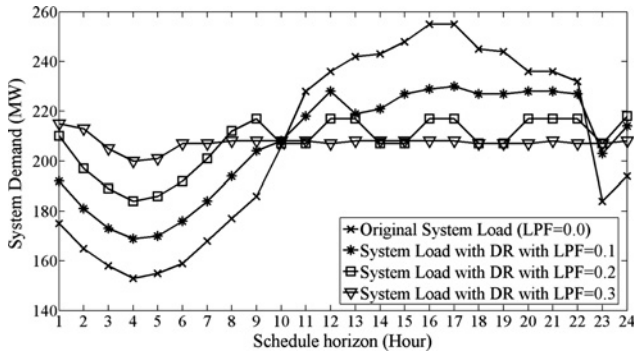


**Fig. 4** *Actual and shifted loads*

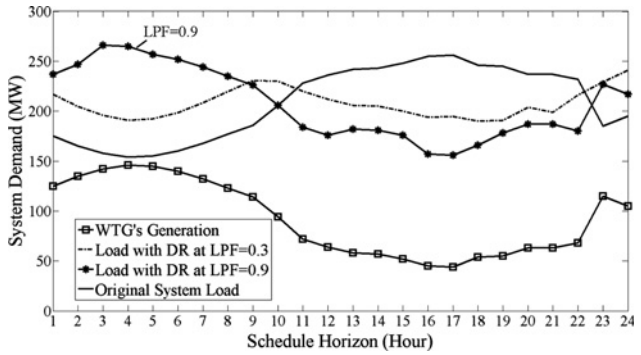


**Fig. 5** *Comparison of WTG output*

output. The scenario reduction method is not applied to this small system. The MCS convergence characteristics for the WTG output and the value of objective function in the 625 scenarios are shown in Fig. 6. The relative error is given as $\left(1.96 \times S_Y/\sqrt{M}\right)/\bar{Y} \times 100\%;$ , where $S_Y$, $M$ and $\bar{Y}$ are standard deviation, number of scenarios and expected value of variable $Y$ under 95% confidence interval, respectively. In Fig. 6, the relative error of the total WTG output with 625 simulations is less than 1.5%, whereas the relative error of objective function is less than 0.2%. Moreover, the relative errors are within 2% after the initial 250 simulations.

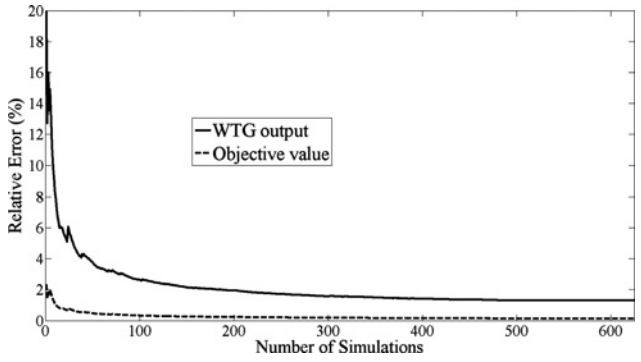


**Fig. 6** *Convergence characteristic of MCS*

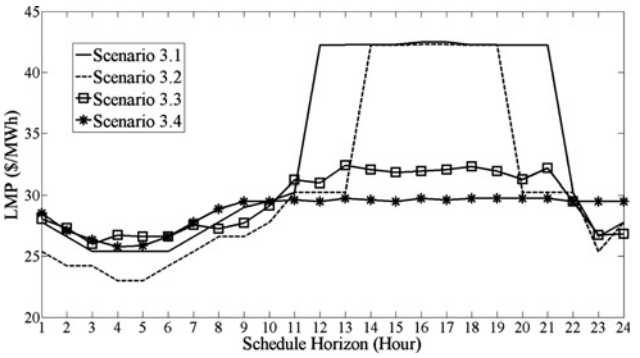


**Fig. 7** *LMPs at Bus 5*

*Case 3*: In this case, the effects of considering DR, WTG variability and storage on the hourly LMP are discussed. We study the following four scenarios in this case:

1. Scenario 3.1: Base case without considering WTG or DR.
2. Scenario 3.2: A variable WTG is considered at Bus 5. The MCS with 625 scenarios used in Case 2 is adopted here.
3. Scenario 3.3: An aggregated and large storage (e.g. pumped storage hydro) located at Bus 5 is added to Scenario 3.2 in order to show explicitly the effect of the storage on hourly LMP profile. The storage parameters are listed in Table 4.
4. Scenario 3.4: DR is considered at Bus 5 based on Scenario 3.2. For comparison, the upper bound of hourly PRL is set to the maximum charge/discharge in Table 4. The pick-up/drop-off rate limits of loads and the minimum up/down times are not considered for load curtailment.

LMPs at bus 5 in the four scenarios are compared in Fig. 7. Here, the LMPs in Scenario 3.1 spike at Hours 12–21. In Scenario 3.2, the time period is shortened to Hours 14–19. However, the peak-valley difference of LMPs becomes larger due to the WTG variability. The price spike in Scenarios 3.3 is mitigated as the storage shifts peak loads to off-peak hours. Scenario 3.4 shows a smoother LMP profile with 1.20 $/MWh of peak-valley LMP difference by shifting loads to off-peak hours. The LMP fluctuations in Scenario 3.4 are reduced as compared to those in Scenario 3.3. A large storage is less effective than DR in reducing the volatility of hourly LMP because the charging of storage may be limited at off-peak hours. Fig. 8 shows the expected hourly storage output against the expected LMP in Scenario 3.3. Here, the storage is charging during low LMP hours and discharging when the LMP is high.

### 5.2 Modified IEEE 118-bus system

The IEEE 118-bus system has 54 thermal generators, 186 branches and 91 load buses. The parameters of generators, transmission network and load profiles are given in [1]. The economic and reliability DR programs at all load buses, random outages of generating unit and transmission lines,

**Table 4** Storage data for 6-bus system

| Capacity, MWh | Max charge, MW | Min charge, MW | Max discharge, MW | Min discharge, MW | Initial SOC, % | Final SOC, % |
|---|---|---|---|---|---|---|
| 300 | 50 | 30 | 50 | 30 | 20 | 20 |

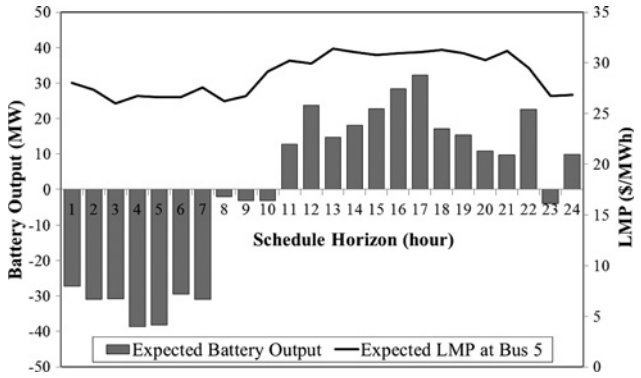


**Fig. 8** *Hourly storage charges against LMP at Bus 5*

load forecast errors, and variable RES, and aggregated storage system are considered. There are three RES including 2 WTGs (at Buses 15,54) and 1 PVA (at Bus 96). A storage with parameters listed in Table 4 is installed at buses with RES. The hourly WTG forecast is provided at http://www.nrel.gov/. VOLL is set at 100 $/MWh. The hourly load forecast error is represented by ±5% of the CBL forecast. We generate 1800 scenarios and reduce the number to 185 by scenario reduction.

Table 5 lists the results in which EXP is the expected value and RERR is the relative error. Here, the expected average LMP is 19.06 ± 0.23 $/MWh with a 0.2 LPF and 20% load shedding. Note that the 19.06 ± 0.23 shows that 5% of LMPs will be beyond the given interval of ±0.23. The smaller the confidence interval, the more accurate will be the expectation. In spite of high VOLL, the load shedding occurs at certain scenarios with transmission line outages. In such scenarios, the average LMP is much higher than that of the base case. In Table 5, the expected average LMP decreases from 19.06 to 18.73 $/MWh as LPF increases from 0.2 to 0.3. In this case, more operating reserves are made available with a higher LPF. The results suggest that the benefit of larger economic DR is more significant when considering system contingencies. The total CPU time is 6.2 h when 185 scenarios are applied. The relative errors of operating cost and average LMP are less than 2% as listed in Table 5. The relative errors will be smaller and the accuracy will be higher if more scenarios are introduced. In such cases, parallel computation can be further adopted in each scenario to reduce the total CPU time.

Fig. 9 shows the reduction in operating costs, average LMPs and load payments as a function of RES contribution, which are compared with the base SCUC (without DR or RES.) In Fig. 9, the reduction in economic metrics increases almost linearly as RES contribution increases. When incorporating a 3.7% RES contribution and a 20% DR, the system operating cost, average LMP and load payment are reduced by 6.93, 17.77 and 20.71%,

**Table 5** DR results with 3 RES (95% confidence interval)

| 20% load shedding | LPF = 0.2 | | LPF = 0.3 | |
|---|---|---|---|---|
| | Operating cost, $ | Average LMP, $/MWh | Operating cost, $ | Average LMP, $/MWh |
| EXP | 1 660 250 ± 22 937 | 19.06 ± 0.23 | 1 652 905 ± 25 193 | 18.73 ± 0.11 |
| RERR | 1.38% | 1.21% | 1.52% | 0.59% |

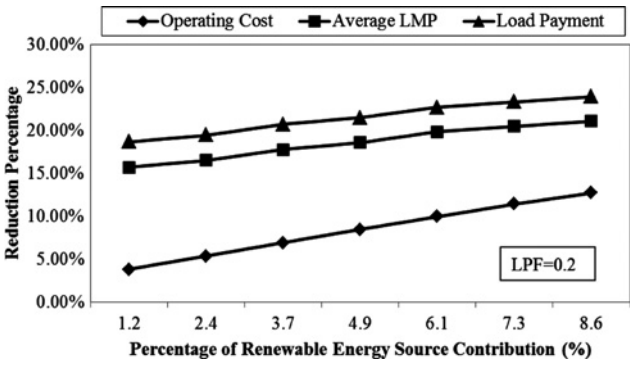


**Fig. 9** *Economic metrics against RES*

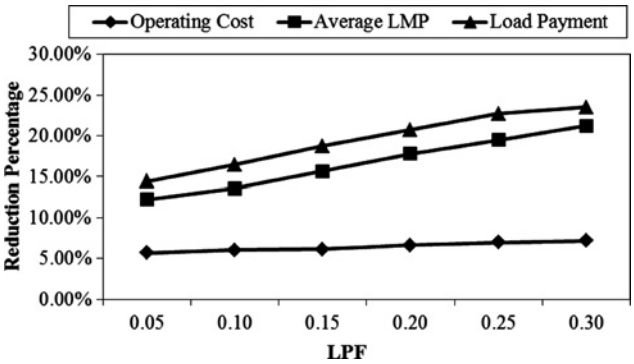


**Fig. 10** *Economic metrics against LPF*

respectively. Fig. 10 shows the variation in economic metrics with LPFs when the RES contribution is 3.7%. Comparing Figs. 9 and 10, it is seen that DR has a higher impact on the reduction of average LMP and load payment, but RES has a higher impact on the reduction of operating cost. The contribution of DR, RES and storage to the average LMP reduction is shown in Fig. 11. In this case, DR is the leading factor in contributing to the 64.3% reduction in the average LMP, which is followed by those of WTG (18.2%), storage (10.4%) and PVA (7.1%).

In Fig. 12, WTG curtailments with or without DR at bus 54 are compared. The expected available wind energy in this case is 24,631 MWh, which is 21.7% of the total daily energy demand. The available wind generation represents the upper limit of actual wind dispatch and the difference between the upper limit and the actual dispatch is defined as wind curtailment. In Fig. 12, the available wind generation is dispatched without any curtailment at Hours 1–13, 18 when the hourly available wind generation is below 232 MW. The lightly shaded area in Fig. 12 shows wind curtailment when considering a 20% DR at Bus 54.

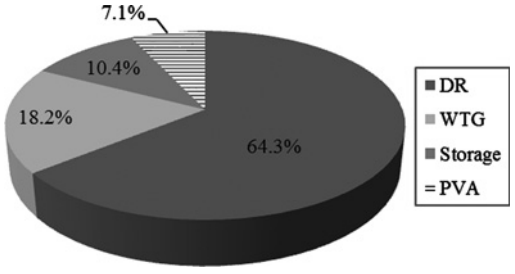


**Fig. 11** *Contribution percentages to average LMP reduction*




doi: 10.1049/iet-gtd.2012.0186

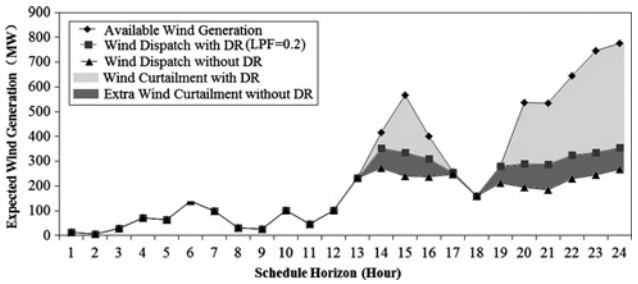


**Fig. 12** *Expected dispatch of WTG at bus 54*

**Table 6** Effect of DR on wind energy in the system

| EXP | Without DR | With DR (LPF = 0.2) |
|---|---|---|
| Total wind curtailment, MWh | 6948 | 4958 |
| Wind penetration, % | 13.4 | 17.3 |

Here, wind curtailment is higher at Hours 14–17, 19–24 when the available wind generation is higher than 256 MW. The flows on Lines 77 and 78, which connect Buses 54–55 and Buses 54–56, reach their respective limits during those curtailment hours. However, when DR is applied, Bus 54 faces a higher wind curtailment without DR, which is represented by darker shade in Fig. 12. This is because the corresponding load can be shifted between hours. Table 6 shows the DR effect on reducing the system wind curtailment. Here, a 20% DR at every load bus would reduce the wind curtailment from 6948 to 4958 MWh, whereas the wind penetration is increased from 13.4 to 17.3%.

## 6 Observations

We list the observations below based on our numerical results.

1. Economic DR offers a flat load profile that leads to lower LMPs, lower transmission congestion and lower system operating cost. Economic DR benefits are more significant when considering system contingencies. Reliability DR provides a chance to maintain the system security.
2. DR has a more significant impact than RES on lowering average LMPs and load payments; RES has a more significant impact than DR on reducing operating costs. DR increases the wind penetration by reducing wind curtailments.
3. The storage system is less effective than DR on lowering the hourly LMP fluctuations which is due to the physical limitation of storage. When compared with RES and storage systems, DR is more effective in reducing average LMPs.

## 7 Conclusions

In this paper, we propose a stochastic optimisation model for the day-ahead power system scheduling, which incorporates the hourly DR for managing the variability of RES. Physical and operating constraints of hourly demand are considered in DR for economic and reliability responses. The MCS creates multiple scenarios for representing possible realisations of uncertainty. Random outages of system components and forecast errors for hourly load and RES are included in MCS. Numerical results demonstrate that DR offers a flat load profile that leads to lower transmission congestions, lower system operating costs and lower LMPs. In addition, DR is the leading factor for lowering LMPs, which outperforms the utilisation of generation resources such as RES and storage. DR increases wind penetration in terms of reducing wind curtailments, which make DR an effective tool for managing the variability of RES.

## 8 Acknowledgment

This study was funded in part by the DOE Award # DE-FC26–08NT02875.

## 9 References

1 Shahidehpour, M., Yamin, H., Li, Z.Y.: 'Market operations in electric power systems' (Wiley, New York, 2002)
2 Albadi, M.H., El-Saadany, E.F.: 'A summary of demand response in electricity markets', *Electr. Power Syst. Res.*, 2008, **78**, (11), pp. 1989–1996
3 U.S. Department of Energy: 'Benefits of demand response in electricity markets and recommendations for achieving them', 2006
4 Conejo, A.J., Morales, J.M., Baringo, L.: 'Real-time demand response model', *IEEE Trans. Smart Grid*, 2010, **1**, (3), pp. 236–242
5 Wang, J., Bloyd, C., Hu, Z., Tan, Z.: 'Demand response in China', *Int. J. Energy*, 2010, **35**, (4), pp. 1592–1597
6 Khodaei, A., Shahidehpour, M., Bahramirad, S.: 'SCUC with hourly demand response considering intertemporal load characteristics', *IEEE Trans. Smart Grid*, 2011, **2**, (3), pp. 564–571
7 Herter, K., McAuliffe, P., Rosenfeld, A.: 'An exploratory analysis of California residential customer response to critical peak pricing of electricity', *Energy*, 2007, **32**, (1), pp. 25–34
8 Valero, S., Ortiz, M., Senabre, C., *et al*: 'Methods for customer and demand response policies selection in new electricity markets', *IET Gener. Transm. Distrib.*, 2007, **1**, (1), pp. 104–110
9 Ummels, B.C., Gibescu, M., Pelgrum, E., Kling, W.L., Brand, A.J.: 'Impacts of wind power on thermal generation unit commitment and dispatch', *IEEE Trans. Energy Convers.*, 2007, **22**, (1), pp. 44–51
10 Atwa, Y.M., El-Saadany, E.F., Salama, M.M.A., *et al*: 'Optimal renewable resources mix for distribution system energy loss minimization', *IEEE Trans. Power Syst.*, 2010, **25**, (1), pp. 360–370
11 Ochoa, L.F., Harrison, G.P.: 'Minimizing energy losses: optimal accommodation and smart operation of renewable distributed generation', *IEEE Trans. Power Syst.*, 2011, **26**, (1), pp. 198–205
12 Mangueira, H.H.D., Saavedra, O.R., Pessanha, J.E.O.: 'Impact of wind generation on the dispatch of the system: a fuzzy approach', *Int. J. Electr. Power Energy Syst.*, 2008, **30**, (1), pp. 67–72
13 Tsikalakis, A.G., Hatziargyriou, N.D., Katsigiannis, Y.A., Georgilakis, P.S.: 'Impact of wind power forecasting error bias on the economic operation of autonomous power systems', *Wind Energy*, 2009, **12**, (4), pp. 315–331
14 Celli, G., Pilo, F.: 'MV network planning under uncertainties on distributed generation penetration'. Proc. 2001 IEEE PES Summer Meeting, vol. 1, pp. 485–490
15 Tuohy, A., Meibom, P., Denny, E., O'Malley, M.: 'Unit commitment for systems with significant wind penetration', *IEEE Trans. Power Syst.*, 2009, **24**, (2), pp. 592–601
16 Meibom, P., Barth, R., Hasche, B., *et al*: 'Stochastic optimization model to study the operational impacts of high wind penetrations in Ireland', *IEEE Trans. Power Syst.*, 2011, **26**, (3), pp. 1367–1379
17 Morales, J.M., Conejo, A.J., Perez Ruiz, J.: 'Economic valuation of reserves in power systems with high penetration of wind power', *IEEE Trans. Power Syst.*, 2009, **24**, (2), pp. 900–910
18 Desrochers, G., Blanchard, M., Sud, S.: 'A Monte Carlo simulation method for the economic assessment of the contribution of wind energy to power systems', *IEEE Trans. Energy Convers.*, 1986, **EC-1**, (4), pp. 50–56
19 Billinton, R., Chen, H., Ghajar, R.: 'A sequential simulation technique for adequacy evaluation of generating systems including wind energy', *IEEE Trans. Energy Convers.*, 1996, **11**, (4), pp. 728–734
20 Billinton, R., Chowdhury, A.A.: 'Incorporation of wind energy conversion systems in conventional generating capacity adequacy assessment', *Proc. Inst. Electr. Eng.-C*, 1992, **139**, (1), pp. 47–56
21 Tina, G., Gagliano, S., Raiti, S.: 'Hybrid solar/wind power system probabilistic modelling for long-term performance assessment', *Sol. Energy*, 2006, **80**, (5), pp. 578–588

22 Day-Ahead Demand Response Program Manual at NYISO. Available at: http://www.nyiso.com/public/webdocs/products/demand_response/day_ahead/dadrp_mnl.pdf

23 Bouffard, F., Galiana, F.D., Conejo, A.J.: 'Market-clearing with stochastic security – Part I: Formulation', *IEEE Trans. Power Syst.*, 2005, **20**, (4), pp. 1818–1826

24 Bouffard, F., Galiana, F.D., Conejo, A.J.: 'Market-clearing with stochastic security – Part II: Case studies', *IEEE Trans. Power Syst.*, 2005, **20**, (4), pp. 1827–1835

25 Karaki, S.H., Chedid, R.B., Ramadan, R.: 'Probabilistic performance assessment of autonomous solar-wind energy conversion systems', *IEEE Trans. Energy Convers.*, 1999, **14**, (3), pp. 766–772

26 Wu, L., Shahidehpour, M., Li, T.: 'Stochastic security-constrained unit commitment', *IEEE Trans. Power Syst.*, 2007, **22**, (2), pp. 800–811

27 Valenzuela, J., Mazumdar, M.: 'Monte Carlo computation of power generation production costs under operating constraints', *IEEE Trans. Power Syst.*, 2001, **16**, pp. 671–677

28 Dupačová, J., Gröwe-Kuska, N., Römisch, W.: 'Scenario reduction in stochastic programming: an approach using probability metrics', *Math. Program.*, 2003, **A 95**, pp. 493–511

29 Wu, H., Guan, X., Zhai, Q., *et al*: 'A systematic method for constructing feasible solution to SCUC problem with analytical feasibility conditions', *IEEE Trans. Power Syst.*, 2012, **27**, (1), pp. 526–534

30 Fu, Y., Shahidehpour, M.: 'Fast SCUC for large-scale power systems', *IEEE Trans. Power Syst.*, 2007, **22**, (4), pp. 2144–2151

31 Guan, X., Xu, Z., Jia, Q.: 'Energy-efficient buildings facilitated by Microgriod', *IEEE Trans. Smart Grid*, 2010, **1**, (3), pp. 2144–2151

32 ILOG CPLEX, ILOG CPLEX Homepage 2009 [Online]. Available at: http://www.ilog.com





doi: 10.1049/iet-gtd.2012.0186